Quantum instability of the flux lines in the coherent state representation

Gonzalo García de Polavieja* and Mark S. Child†
Physical and Theoretical Chemistry Laboratory, South Parks Road, Oxford OX1 3UB, United Kingdom
(Received 28 May 1996)

Instability as the exponential divergence of initially neighboring flux lines of the coherent state representation of quantum mechanics is shown to reduce in the classical limit to the standard definition of classical instability. The equations for the coherent state flux lines are derived and the proposed definition for quantum instability is shown to be of practical utility by numerical analysis of the double well potential under a monochromatic external driving force. Regular and chaotic flux lines are found in accordance with the classical trajectories. [S1063-651X(97)10702-4]

PACS number(s): 05.45.+b, 03.65.−w

I. INTRODUCTION

Conceptual and practical problems in quantum theory have often been related to finding the quantum counterpart of a classical phase space trajectory. The interpretation of quantum theory, the tunneling times through a potential barrier, and quantum chaos studies have largely been related to this problem. Decoherent histories [1], Nelson stochastic paths [2], and Bohmian trajectories [3] play an important role in the interpretational problem of quantum theory. Feynman paths and Bohmian and Wigner trajectories are some of the important proposals to the tunneling time problem [4]. The quantum chaos problem, that is, finding the quantum counterpart of classically chaotic motion, has been largely influenced by Feynman paths and semiclassical theories [5,6] and have made important contributions in atomic and molecular physics [6].

The most important advances in the study of quantum counterparts of classical chaos have been related to finding the quantum properties of classically chaotic systems (quantum chaology studies [7]). Concerning the problem of finding the quantum counterpart of classical chaos, the standard answer is that it does not exist in relation to the Schrödinger equation and that it may take place in the measurement process as the measurement apparatus is a classical object and due to the collapse process [8]. Some have looked for new definitions in classical mechanics that could be carried over to quantum mechanics. In this respect information theory and algorithmic entropy have played a prominent role [9–11]. Other proposals have retained the standard definition of classical instability as the exponential divergence of initially neighboring trajectories in phase space and have sought for its quantum counterpart. Mendes [12] proposed deformations outside Hilbert space and Kanno and Ishida [13] considered the separation of Feynman paths. However, what is clearly needed is to treat the problem as a particular problem of the foundations of quantum theory. Along this line, Dürr, Goldstein, and Zanghi [14] have argued that quantum chaos arises naturally in Bohmian mechanics. One of us [15] has found that Bohmian trajectories separate linearly or exponentially for a typical nonintegrable system depending on the initial conditions in accordance with the classical solution.

In this paper we use a causal dynamics recently proposed by one of us as a new interpretation of quantum theory [16,17] that offers a physical insight different from Bohmian mechanics. For a given wave function, in Bohmian mechanics there is one possible momentum for a given position at time t. In the dynamics we consider here all initial momenta are available with different probabilities and in the classical limit the probability is peaked on the classically available momenta. The difference is more striking in the case of stationary states of bound systems for which Bohmian mechanics describes the particle as standing still whereas in our case the particle moves and with classical mechanics as a limit. Therefore, in our dynamics there can be chaotic motion in the stationary states as well as in nonstationary wave functions. The causal dynamics we propose to consider are mathematically described by the flux lines of the coherent state representation of quantum mechanics, which we argue must reduce to phase space classical trajectories in the classical limit (which are the flux lines of the Liouville equation). Thus by defining quantum instability as the exponential separation of flux lines in the coherent state representation of quantum mechanics, we recover the standard definition of classical instability in the classical limit. Equations for the relevant flux lines in the coherent state representation of quantum mechanics are given in Sec. II, where it is argued that the classical limit of the flux lines for the appropriate ensemble are the phase space classical trajectories. In Sec. III we propose to define quantum instability as the exponential separation of flux lines in the coherent state representation of quantum mechanics. This definition of quantum instability reduces to the standard definition of classical instability in the classical limit. In Sec. IV we show the utility of this definition of quantum instability by numerically obtaining the coherent state flux lines for a double well potential under a monochromatic external driving force. Regular and chaotic flux lines are studied. Conclusions are given in Sec. V.

II. COHERENT STATE FLUX LINES

The coherent state representation, as defined by the transformation [18]

*FAX: Oxford (01865) 275410. Electronic address: gonzalo@rydberg.thchem.ox.ac.uk
†Electronic address: childms@vax.ox.ac.uk

$$\langle q,p|\psi\rangle=\left(\frac{\lambda}{2\pi}\right)^{1/4}\int dx\langle x|\psi\rangle \times\exp\left[-\frac{\lambda}{2\hbar}(x-q)^2-\frac{i}{\hbar}p(x-q)\right] \quad (1)$$

has been shown by Torres-Vega and Frederik [19] to satisfy the Schrödinger equation

$$i\hbar\frac{\partial}{\partial t}\langle q,p|\psi\rangle=\langle q,p|\hat{H}(\hat{Q},\hat{P})|\psi\rangle \quad (2)$$

in which the operators $\hat{Q}$ and $\hat{P}$ take the form

$$\langle q,p|\hat{Q}|\psi\rangle=(q+i\hbar\nabla_p)\langle q,p|\psi\rangle, \quad (3a)$$

$$\langle q,p|\hat{P}|\psi\rangle=-i\hbar\nabla_q\langle q,p|\psi\rangle. \quad (3b)$$

Alternative forms are also possible, because it is readily demonstrated that

$$\nabla_q\langle q,p,|\psi\rangle=\left(i\lambda\nabla_p+\frac{p}{\hbar}\right)\langle q,p|\psi\rangle, \quad (4)$$

but Eqs. (3) have the convenience that they are independent of λ. It is assumed in what follows that the Hamiltonian operator is of the form

$$\hat{H}=\frac{1}{2m}\hat{P}^2+V(\hat{Q}). \quad (5)$$

Inserting the polar form $\langle q,p|\psi\rangle=R(q,p,t)e^{(i/\hbar)S(q,p,t)}$ for the wave function in Eq. (2) and separating real and imaginary parts, we obtain the following two equations:

$$-\frac{\partial S}{\partial t}=\frac{(\nabla_q S)^2}{2m}-\frac{\hbar^2}{2m}\frac{\nabla_q^2 R}{R} +\frac{1}{R}\mathrm{Re}[e^{-(1/\hbar)S}V(q+i\hbar\nabla_p)Re^{(i/\hbar)S}], \quad (6)$$

$$\frac{\partial R^2}{\partial t}+\nabla_q\left[R^2\left(\frac{\nabla_q S}{m}\right)\right] -\frac{2}{\hbar}\mathrm{Im}[Re^{-(1/\hbar)S}V(q+i\hbar\nabla_p)Re^{(i/\hbar)S}]=0. \quad (7)$$

There is some ambiguity in the interpretation of Eqs. (6) and (7), because the partial derivatives of S and R are interrelated by Eq. (4) but the relationship to classical mechanics is best revealed by use of the identities

$$\nabla_q S=p+\lambda\hbar\frac{\nabla_p R}{R}, \quad (8a)$$

$$\nabla_p S=-\frac{\hbar}{\lambda}\frac{\nabla_q R}{R}. \quad (8b)$$

Taken together with the binomial expansion

$$(q+i\hbar\nabla_p)^n=\sum_{r=0}^{n}\frac{n!}{r!(n-r)!}q^{n-r}(i\hbar\nabla_p)^r \quad (9)$$

it follows for a potential of the general form $V(Q)=\Sigma_n a_n Q^n$ that Eqs. (6) and (7) go over to

$$-\frac{\partial S(q,p,t)}{\partial t}=\frac{p^2}{2m}+V(q)+W(q,p,t), \quad (10)$$

$$\frac{\partial R^2(q,p,t)}{\partial t}+\nabla_q\left[\frac{p}{m}R^2(q,p,t)\right]+\nabla_p\{[-\nabla_q V(q)+Z(q,p,t)]R^2(q,p,t)\}=0, \quad (11)$$

with

$$W(q,p,t)=W_1(q,p,t)+W_2(q,p,t), \quad (12a)$$

$$W_1(q,p,t)=-\frac{\hbar^2}{2m}\frac{\nabla_q^2 R}{R}+\frac{\lambda\hbar}{m}p\frac{\nabla_p R}{R}+\frac{\lambda^2\hbar^2}{4m}\frac{(\nabla_p R)^2}{R^2}, \quad (12b)$$

$$W_2(q,p,t)=\sum_n\frac{a_n}{R}\mathrm{Re}\left[e^{-(i/\hbar)S}\left(\sum_{r=1}^{n}\frac{n!}{r!(n-r)!}q^{n-r}(i\hbar\nabla_p)^r\right)Re^{(i/\hbar)S}\right] \quad (12c)$$

and

$$Z(q,p,t)=Z_1(q,p,t)+Z_2(q,p,t), \quad (13a)$$

$$Z_1(q,p,t)=-\frac{2}{\hbar R^2}\int dp\sum_n a_n\mathrm{Im}\left[Re^{-(i/\hbar)S}\left(\sum_{r=2}^{n}\frac{n!}{r!(n-r)!}q^{n-r}(i\hbar\nabla_p)^r\right)Re^{(i/\hbar)S}\right], \quad (13b)$$

$$Z_2(q,p,t)=\frac{\lambda\hbar}{m}\frac{\nabla_q R}{R}=-\frac{\lambda^2}{m}\nabla_p S. \tag{13c}$$

Equations (10) and (11) are equivalent to the Schrödinger equation in the coherent state representation in Eq. (2) provided that $R(q,p,t)$, $S(q,p,t)$, and their derivatives are continuous and single valued over the phase space.

We concentrate on Eq. (11), which is a continuity equation in phase space. The flux lines of this equation are the solution $(q(t),p(t))$ of the differential equations

$$\dot{q}=\frac{p}{m}, \tag{14}$$

$$\dot{p}=-\nabla_q V(q)+Z(q,p,t), \tag{15}$$

with $Z(q,p,t)$ given by Eq. (13). To obtain the trajectory $(q(t),p(t))$, the initial values $(q(0),p(0))$ must be supplied as input. An initial ensemble of points consistent with the initial quantum probability density moving under the flux equations (14) and (15) will reproduce the quantum probability density for all times due to the existence of the phase space continuity equation (11), as in the de Broglie–Bohm quantum theory of motion [20]. Note that the equations for the flux lines of the coherent state representation of quantum mechanics are not unique. For example, using relation (8a) we can move the Z_2 term, Eq. (13d), to the $\dot{q}$ term in Eq. (14) and still obey the continuity equation (11). Test calculations in the different gauges have shown that the following stability analysis is largely independent of the gauge.

It is clear from Eqs. (14) and (15) that the equations of motion for the flux lines reduce to the classical Hamiltonian form if

$$Z(q,p,t)=0 \tag{16}$$

for all q, p, and t sampled by the ensemble. The resulting coincidence between coherent state flux lines and classical phase space trajectories does not, however, alone correspond to the classical limit. It is also necessary that Eq. (10) above correspond to the classical energy; in other words, $W(q,p,t)=0$ for the appropriate ensemble. Analysis of the harmonic oscillator case in the Appendix shows that the classical limit is reached in this case because $Z(q,p,t)=0$ and secondly because the proper ensemble progressively peaks around the classical orbit and where alone $W(q,p,t)=0$.

III. INSTABILITY OF CLASSICAL AND QUANTUM FLUX LINES

In classical mechanics, instability is defined as the exponential divergence of initially neighboring trajectories in phase space. Lyapunov exponents and Kolmogorov entropies are used as measures of this exponential separation [21]. We propose by analogy to define instability in quantum theory as the exponential divergence of initially neighboring coherent state flux lines, in order to recover the classical definition in the classical limit when coherent state flux lines reduce to the phase space classical trajectories, that is, to the flux lines of the corresponding Liouville equation. We note that the form of the equations of motion for quantum flux lines, Eqs. (14) and (15), are highly nonlinear, as can be clearly seen from the form of $Z(q,p,t)$ in Eq. (13). Hence the behavior of the coherent state flux lines is expected to be more complex than that of the classical trajectories, but the degree of nonlinearity must reduce to that of classical mechanics in the classical limit.

IV. COHERENT STATE FLUX LINES IN THE DRIVEN DOUBLE WELL POTENTIAL

In this section we show how the above definition of quantum instability can be used to distinguish regular and chaotic motion in quantum mechanics. We present numerical calculations for a particle in a double well potential under a monochromatic external driving force, as defined by the Hamiltonian

$$H=\frac{P^2}{2m}+AQ^4-BQ^2+\sigma Q\ \cos\omega_0 t. \tag{17}$$

The classical dynamics for this Hamiltonian is known to be regular or chaotic depending on the initial conditions and the value of the coupling parameter σ. Previous quantum mechanical studies have been made by Lin and Ballentine [22] who examined the evolution of initially minimum uncertainty wave packets in the coherent state representation for different wave packet centers and different values of the coupling parameter. Expectation values and the rms uncertainty were also discussed by Lin and Ballentine and compared with the classical solution. Implications for the enhancement and reduction of tunneling for this system have also been discussed by these authors and by Grossmann *et al.* [23].

In the following we briefly describe our numerical calculations. Eigenstates were calculated by numerically diagonalizing a 100×100 matrix of the Hamiltonian in a harmonic oscillator basis set, for which the coherent state representation has a known analytical form (see Appendix). The parameters of the Hamiltonian were chosen to make contact with the results of Lin and Ballentine [22], $m=1$, $A=0.5$, $B=10$, $\hbar=1$ and initially minimum uncertainty wave packets with variance of $(\Delta\hat{x})=0.08$. The wave packet dynamics were calculated by expansion in the eigenstates basis as

$$\langle q,p|\Psi\rangle=\sum_n \langle q,p|n\rangle\langle n|\Psi(0)\rangle\exp\left\{-\frac{i}{\hbar}E_n t\right\}, \tag{18}$$

which holds for all times for the zero coupling parameter case, $\sigma=0$, and for times obeying $t=j\tau$ with τ the period of the driving force and j an integer for the nonzero coupling parameter cases, $\sigma\neq0$. For this last case n and E_n stand for Floquet eigenstates and Floquet quasienergies, respectively. Coherent state flux lines were obtained by solving Eqs. (14) and (15) by a fourth order Runge-Kutta method. For nonzero values of the coupling parameter we have, for numerical efficiency, considered the wave packet to be frozen between times corresponding with the period of the driving force. Of course, the eigenfloquet expansion in Eq. (18) guarantees a correct representation of the wave packet for times equal to multiples of the period of the driving force.

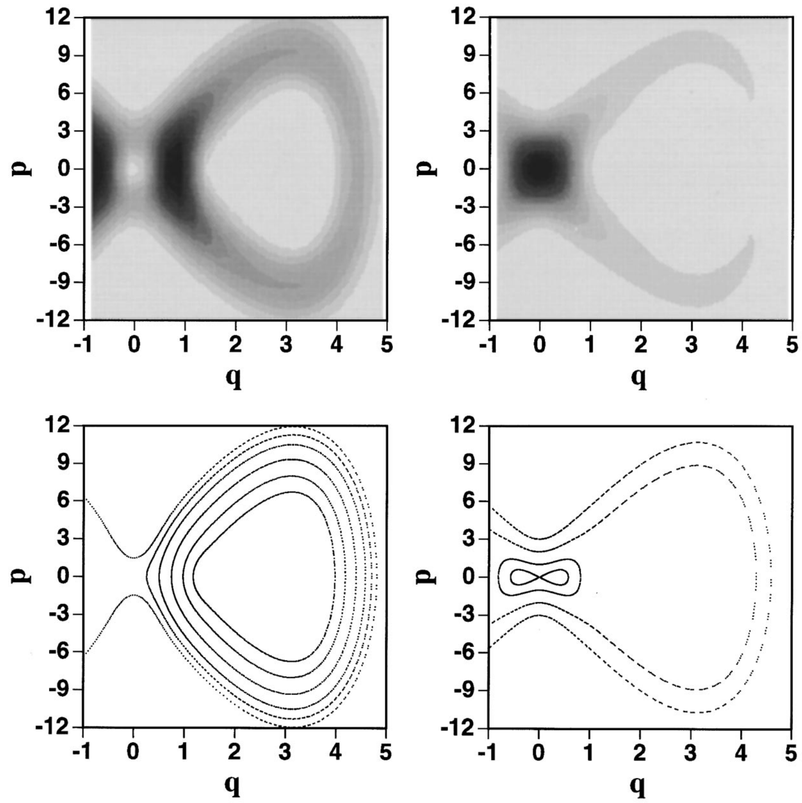

FIG. 1. Density plots of the coherent state probability density of an odd (left) eigenstate and an even (right) eigenstate close to the unstable point of the undriven double well potential (upper pannel). Some of the corresponding flux lines are plotted in the lower pannel.

Before studying the results for wave packet dynamics, we discuss the coherent state flux lines for the simpler case of two eigenstates close to the unstable point of the undriven double well potential with $\sigma=0$. In Fig. 1 we present the 18th (odd) and 19th (even) eigenstates in the coherent state representation with eigenenergies $E_{18}=-3.542$ and $E_{19}=-0.327$. The odd eigenstate is localized mainly on the classical separatrix with the exception of the hyperbolic point, while the even eigenstate is concentrated mainly on the hyperbolic point. This is a simple case of the ''scar'' phenomenon [24] of quantum localization onto a classically unstable periodic orbit. These features can also be studied in the corresponding coherent state flux lines in Fig. 1. For most members of the ensemble, the flux lines for the even state mainly describe oscillations around or close to the hyperbolic point while for the odd case they reproduce motions close to the separatrix motion but avoid the hyperbolic point.

Results for wave packet dynamics are presented for three different parameter sets, which correspond to (a) regular classical motion for $\sigma=0$, (b) chaotic classical motion for most initial conditions for $(\sigma,\omega_0)=(6,5.35)$, and (c) regular or chaotic motion depending on the initial conditions for $(\sigma,\omega_0)=(3,5.35)$. Figure 2 shows the classical stroboscopic maps for cases (b) and (c), which will serve for comparison with our quantum results.

In Fig. 3 we show the coherent state flux lines for wave packets corresponding to cases (a), (b), and (c). On the left, the values of position and momentum of the flux lines are displayed and on the right the time dependence of the variable q. For case (a) with $\sigma=0$ the wave packet is centered at $(\overline{q,p})=(3.0,0.1)$ and the initial value for the flux line is at the same phase space point, $(q(0),p(0))=(3.0,0.1)$. The behavior can be seen to be very similar to that of the classical solution and approach that of a harmonic oscillator motion near the minimum of the right hand well (see Appendix).

This behavior is in clear contrast to that of case (b), with $(\sigma,\omega_0)=(6,5.35)$. In this case the wave packet is centered at $(\overline{q,p})=(0.1,4.5)$ and the initial value for the flux line is also at that point, $(q(0),p(0))=(0.1,4.5)$. The phase space dynamics of the flux lines and the time series behave in a complicated way. An interesting feature of this irregular case is the short term localization, which can already be seen in the parabolic barrier case [20]. In case (c), with the parameter values $(\sigma,\omega_0)=(3,5.35)$, the dynamical behavior of the flux lines is richer than the two preceding cases. The wave packet is centered at $(\overline{q,p})=(-3.1,0.1)$ and the initial value for the flux line is also at $(q(0),p(0))=(-3.1,0.1)$. The flux line has a rather regular behavior, although more complicated than in the integrable case (a) up to time $t=50$, but thereafter the dynamics change drastically. The flux line *tunnels* from the left well to the right well and returns to the left well again. In the classical case the phase space region through

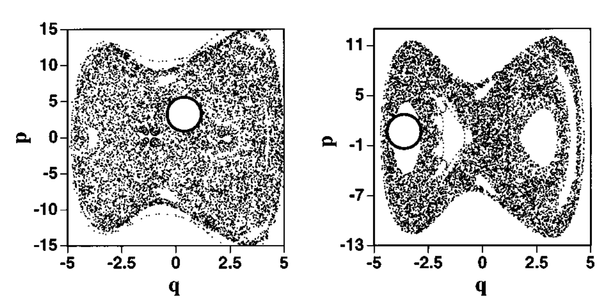

FIG. 2. Stroboscopic maps for the driven double well potential with potential parameters $(\sigma,\omega_0)=(6,5.35)$ on the left plot and $(\sigma,\omega_0)=(3,5.35)$ on the right plot. Thick circles indicate the location of initial wave packets.

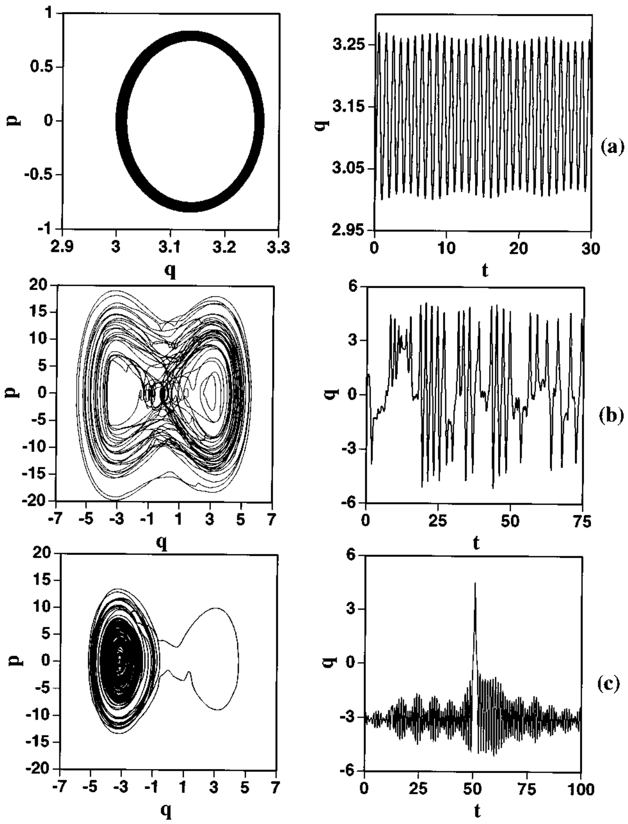

FIG. 3. Coherent state flux lines and time development of the position value for wave packets initially located in (a) a classically regular region for $\sigma=0$, (b) a classically chaotic region for potential parameters $(\sigma,\omega_0)=(6,5.35)$, and (c) a classically regular region for potential parameters $(\sigma,\omega_0)=(3,5.35)$ corresponding to a classically mixed phase space.

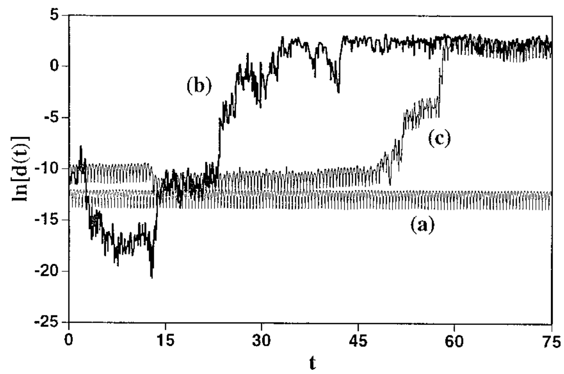

FIG. 4. Natural logarithm of the separation in time of the flux lines in cases (a), (b), and (c) of Fig. 3 with flux lines initially separated 10^{-5} in q and p.

which the flux lines is *tunneling* is chaotic (see Fig. 2) and we will see in the following that tunneling through a classically chaotic region affects the stability of the coherent state flux line.

In order to study the stability of the flux lines, we have analyzed the behavior of flux lines initially very close to the regular, chaotic, and mixed ones already studied. Figure 4 presents the natural logarithm of the phase space distance $d(t)$ between the flux lines studied in Fig. 3 and flux lines initially separated by 10^{-5} in q and p. Case (a) corresponds with the regular case in which the separation of flux lines is clearly not exponential. Case (b) corresponds to the irregular case and it can be clearly seen that the global separation is exponential. Therefore, this case is unstable in the same sense as the classical solution. In case (c) the separation is not exponential until time $t=50$ at which the separation begins to be exponential with a slope very similar to that of case (b). This time corresponds to the *tunneling* of the flux line through a classically chaotic region. We have observed that this behavior is general for those cases in which the classical dynamics is regular or chaotic depending on the initial conditions. The flux lines then display regular and chaotic inserts in their evolution.

To conclude, we have derived the quantum mechanical coherent state flux equations and proposed a definition of instability analogous to that used in classical mechanics. The distinguishing feature of our approach is that the coherent state flux lines reduce to phase space classical mechanics in the classical limit; hence our definition of quantum instability goes over the standard one in classical mechanics. Numerical calculations of coherent state flux lines in a driven double well potential have shown that the definition proposed is of practical value in the study of regular and chaotic solutions in quantum mechanics. We have also shown that in the general case where we have tunneling between regions of different classical stability the local stability of the flux lines change with time.

ACKNOWLEDGMENTS

G.G. acknowledges an EC Research Training Grant.

APPENDIX

In this Appendix we give the solution of the flux lines in the coherent state representation and the expression for the energy for the stationary and nonstationary cases of the harmonic oscillator. Further discussion can be found in [16,17].

The coherent state representation of the eigenfunction for a harmonic oscillator with Hamiltonian $H=P^2/2m+\frac{1}{2}m\omega^2Q^2$ *is*

$$\langle q,p|\Psi_n\rangle=N_n'\left(\frac{\epsilon}{\hbar\omega}\right)^{n/2}\exp\left(-\frac{\epsilon}{2\hbar\omega}+in\,\tan^{-1}\left(-\frac{1}{m\omega}\frac{p}{q}\right)+\frac{i}{\hbar}\frac{pq}{2}-\frac{i}{\hbar}E_nt\right) \tag{19}$$

with $\epsilon=(p^2/2m+\frac{1}{2}m\omega^2q^2)$ and the eigenenergy $E_n=(n+\frac{1}{2})\hbar\omega$. The equations of motion for the flux lines and the energy, Eqs. (14), (15), and (10) reduce in this case to

$$\dot{q}=\frac{p}{m}, \tag{20}$$

$$\dot{p}=-m\omega^2q, \tag{21}$$

$$E=E_n. \tag{22}$$

The differential equation for the flux lines (20) and (21) coincide with the classical ones. However, the energy has the value of the eigenenergy irrespective of the initial conditions, which has its classical relationship with position and momentum for the phase space loop $\epsilon = E_n$ whereas the distribution $|\langle q,p|\Psi\rangle|^2$ is maximum at $\epsilon = n\hbar\omega$. The energy difference between these two phase space loops is of $\hbar\omega/2$. The classical limit for all members of the ensemble is approached at high n corresponding to a phase space distribution concentrated on the $\epsilon = n\hbar\omega$ loop and for which the $\hbar\omega/2$ contribution to the energy is negligible.

The coherent state representation of the coherent wave packet is of the form

$$\langle q,p|\psi\rangle = (2\pi\hbar)^{-1/2} \exp\left(-\frac{m\omega}{4\hbar}(q-x_t)^2 - \frac{1}{4\hbar m\omega} \times (p-p_t)^2 + \frac{i}{2\hbar}\{qp_t - px_t\} + \frac{i}{\hbar}\frac{pq}{2} - \frac{i}{2}\omega t \right) \tag{23}$$

with

$$x_t = x_0\cos(\omega t) + \frac{1}{m\omega}p_0\sin(\omega t), \tag{24}$$

$$p_t = p_0\cos(\omega t) - m\omega x_0\sin(\omega t). \tag{25}$$

The equations for the coherent state flux lines (14) and (15) for this case also reduce to the classical equations but the energy of the particle in Eq. (10) reduces to

$$E = \frac{pp_t}{2m} + \frac{1}{2}m\omega^2(qx_t) + \frac{\hbar\omega}{2}, \tag{26}$$

with x_t and p_t given by (24) and (25). For the center of the wave packet the expression for the energy in Eq. (26) reduces to

$$E = \frac{p_t^2}{2m} + \frac{1}{2}m\omega^2 x_t^2 + \frac{\hbar\omega}{2}, \tag{27}$$

which has a constant quantum contribution to the classical energy of $\hbar\omega/2$. The classical limit is obtained for high energy for which the constant contribution to energy is negligible.

[1] R. B. Griffiths, Phys. Rev. Lett. **70**, 2201 (1993); R. Omnès, Rev. Mod. Phys. **64**, 339 (1992); M. Gellmann and J. B. Hartle, in *Complexity, Entropy and the Physics of Information*, edited by W. Zurek (Addison-Wesley, Reading, 1990).

[2] E. Nelson, Phys. Rev. **150**, 1079 (1966); *Quantum Fluctuations* (Princeton University Press, Princeton, 1985).

[3] D. Bohm and B. J. Hiley, *The Undivided Universe* (Routledge, New York, 1993); P. R. Holland, *The Quantum Theory of Motion* (Cambridge University Press, Cambridge, 1993).

[4] R. Landauer and Th. Martin, Rev. Mod. Phys. **66**, 217 (1994).

[5] M. C. Gutzwiller, *Chaos in Classical and Quantum Mechanics* (Springer-Verlag, Berlin, 1990).

[6] M. S. Child, *Semiclassical Mechanics with Molecular Applications* (Oxford University Press, Oxford, 1991).

[7] M. V. Berry, Proc. R. Soc. London Ser. A **243**, 219 (1989).

[8] G. Casati and B. Chirikov, in *Quantum Chaos*, edited by G. Casati and B. Chirikov (Cambridge University Press, Cambridge, 1995).

[9] J. Ford and G. Mantica, Am. J. Phys. **60**, 1086 (1992).

[10] R. Schack and C. Caves, Phys. Rev. Lett. **71**, 525 (1992).

[11] W. H. Zurek and J. P. Paz, Phys. Rev. Lett. **72**, 2508 (1994).

[12] R. V. Mendes, Phys. Lett. A **171**, 253 (1992).

[13] R. Kanno and A. Ishida, J. Phys. Soc. Jpn. **63**, 2902 (1994).

[14] D. Dürr, S. Goldstein, and N. Zanghi, J. Stat. Phys. **68**, 259 (1992).

[15] G. García de Polavieja, Phys. Rev. A **53**, 2059 (1996).

[16] G. García de Polavieja, Phys. Lett. A **220**, 303 (1996).

[17] G. García de Polavieja, Found. Phys. Lett. (to be published).

[18] *Coheret States*, edited by J. R. Klauder and Skagerstum (World Scientific, Singapore, 1985).

[19] Go. Torres-Vega and J. H. Frederik, J. Chem. Phys. **93**, 8862 (1990).

[20] K. Berndl, D. Dürr, S. Goldstein, G. Peruzzi, and N. Zanghi, Commun. Math. Phys. **173**, 647 (1995).

[21] G. Nicolis, *Introduction to Nonlinear Science* (Cambridge University Press, Cambridge, 1995).

[22] W. A. Lin and L. E. Ballentine, Phys. Rev. Lett. **65**, 2927 (1990); Phys. Rev. A **45**, 3637 (1992).

[23] F. Grossmann, T. Dittrich, P. Jung, and P. Hanggi, Phys. Rev. Lett. **67**, 516 (1991).

[24] E. J. Heller, Phys. Rev. Lett. **53**, 1515 (1984).